

## Supporting Information

# Calibration-Free Parallel Transmission of the Cervical, Thoracic, and Lumbar Spinal Cord at 7T

Christoph S. Aigner<sup>1</sup>, Manuel F. Sánchez Alarcon<sup>1,2</sup>, Alexandre D'Astous<sup>3,6</sup>, Eva Alonso-Ortiz<sup>3,6</sup>, Julien Cohen-Adad<sup>3,4,5,6</sup>, Sebastian Schmitter<sup>1,7,8</sup>

<sup>1</sup>Physikalisch-Technische Bundesanstalt (PTB), Braunschweig and Berlin, Germany

<sup>2</sup>Working Group on Cardiovascular Magnetic Resonance, Experimental and Clinical Research Center, a joint cooperation between the Charité Medical Faculty and the Max-Delbrück Center for Molecular Medicine, Berlin, Germany

<sup>3</sup>NeuroPoly Lab, Institute of Biomedical Engineering, Polytechnique Montréal, Montréal, Quebec, Canada.

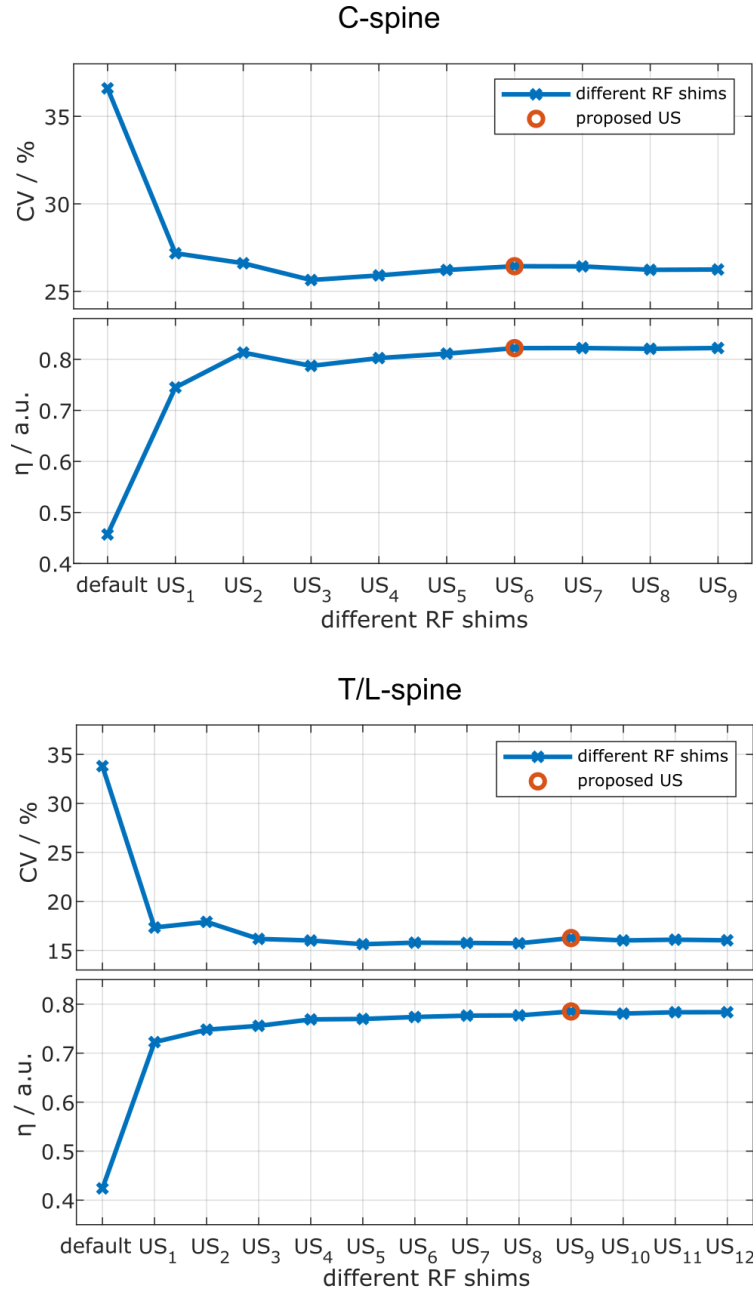
<sup>4</sup>Functional Neuroimaging Unit, CRIUGM, Université de Montréal, Montréal, Quebec, Canada.

<sup>5</sup>Mila-Quebec AI Institute, Montréal, Quebec, Canada.

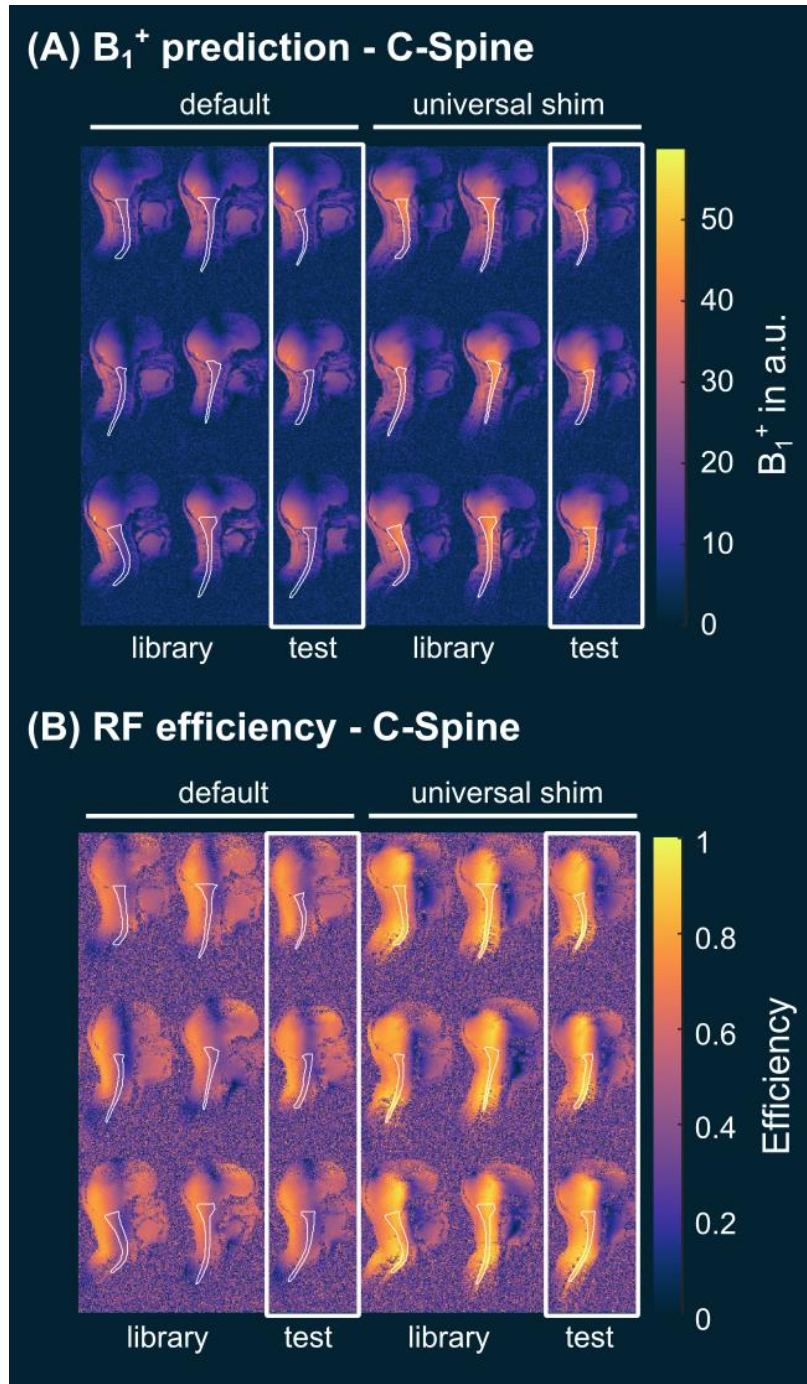
<sup>6</sup>Centre de recherche du CHU Sainte-Justine, Université de Montréal, Montréal, Quebec, Canada.

<sup>7</sup>Medical Physics in Radiology, German Cancer Research Center (DKFZ), Heidelberg, Germany

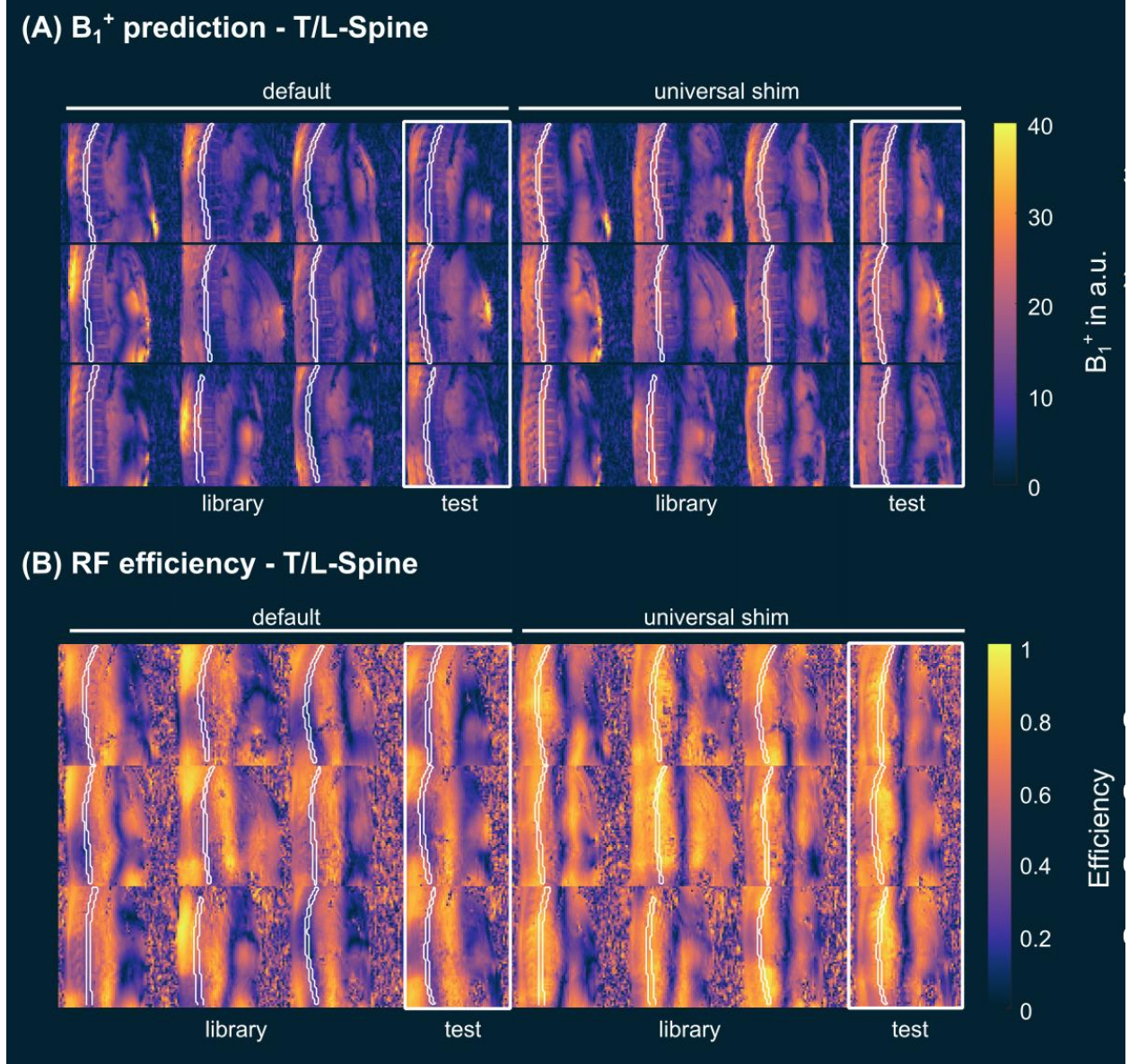
<sup>8</sup>Center for Magnetic Resonance Research, University of Minnesota, Minneapolis, MN, United States



Supporting Information Figure S1: Retrospective simulation study that shows the impact of different library sizes on the RF shim performance in terms of  $B_1^+$  transmit homogeneity measured by the Coefficient of Variation (CV) and the  $B_1^+$  transmit efficiency ( $\eta$ ). The subscript indicates how many different subjects were included in the pulse design. All RF shims were evaluated on all subjects (9 for the C-spine and 12 for the TL-spine). In the experimental validation, we measured the absolute B1+ maps with the two proposed universal shims (US6 for the C-spine and US9 for the TL-spine) and the two default RF shim configurations.

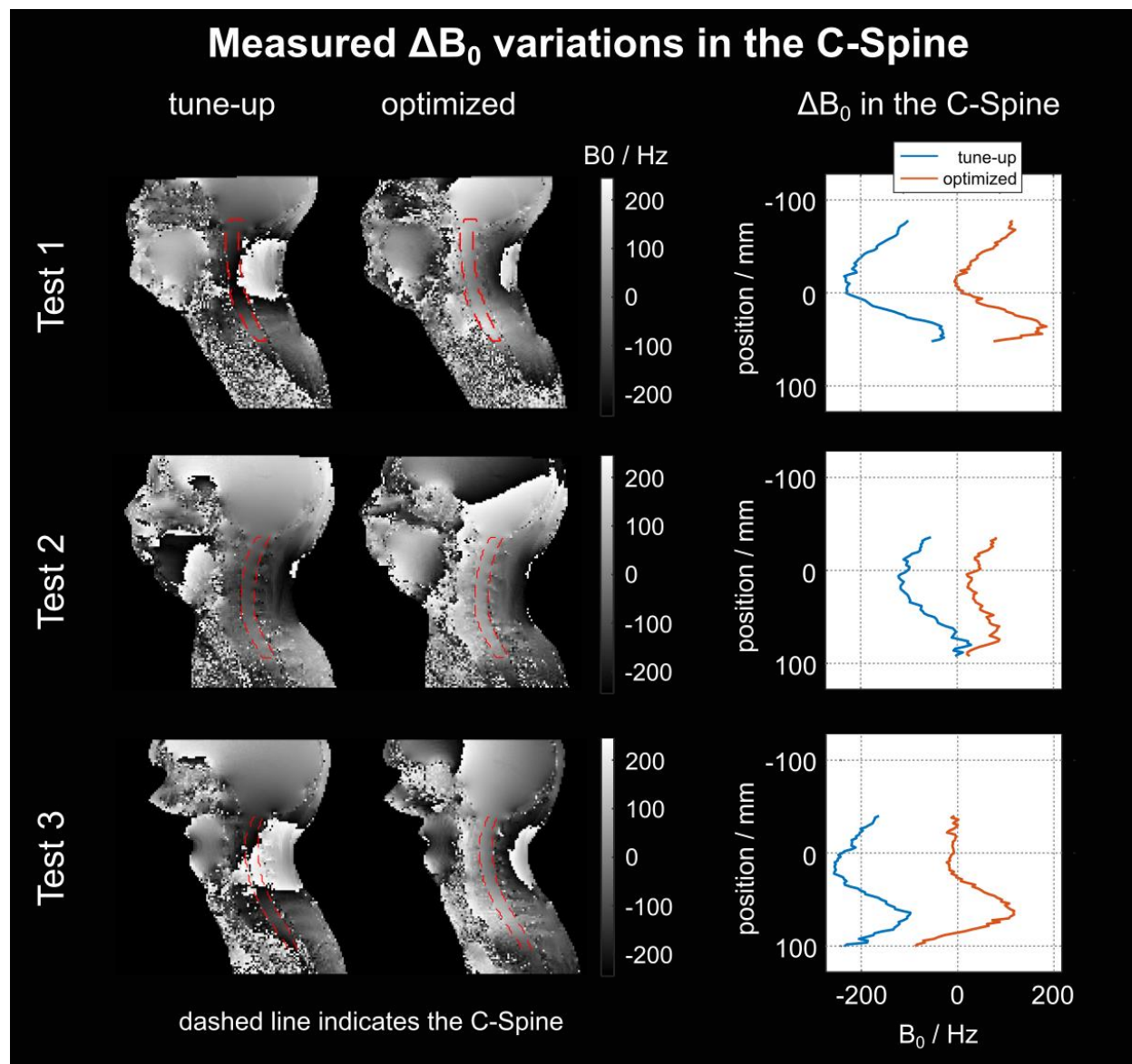


Supporting Information Figure S2: Prediction (A) and RF efficiency (B) in a single sagittal slice utilizing the default shim setting and the optimized universal phase shim specifically designed for the six C-spine regions from the library. The Universal Shim (US) outperforms the default shim with lower coefficient of variation (CV) (36% vs. 26%) and significantly increased RF efficiency (0.46 vs. 0.82) across the library and test cases, resulting in nearly a two-fold increase in the  $B_1^+$  values.

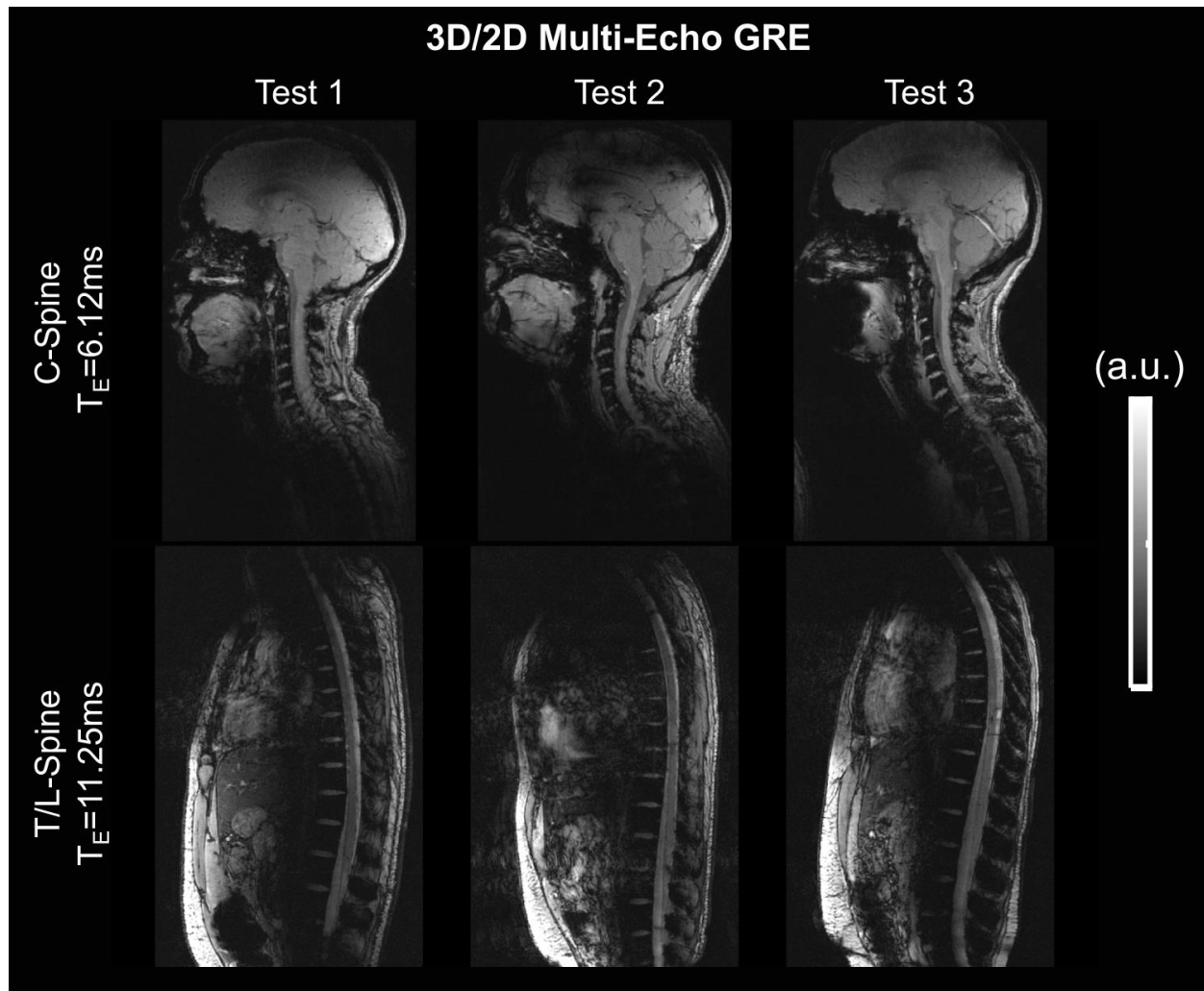


Supporting Information Figure S3:  $B_1^+$  prediction (A) and RF efficiency (B) in a single sagittal slice utilizing the default shim setting and the optimized universal phase shim specifically designed for the nine TL-spine regions from the library. The Universal Shim (US) outperforms the default shim with lower coefficient of variation (CV) (34% vs. 16%) and significantly increased RF efficiency (0.42 vs. 0.78) across the library and test cases, resulting in nearly a two-fold increase in the  $B_1^+$  values.





Supporting Information Figure S4: Measured GRE-based field map of a single sagittal slice, selected from a 3D volume, utilizing the Universal Shim setting in the C-spine of the three test cases, both before and after 2nd order  $B_0$  shimming to address magnetic field inhomogeneities within the spinal cord. The shim volume is outlined with a dashed line and was performed for the entire 3D SC volume using the SC Shimming Toolbox. The unshimmed and shimmed field maps unveil persistent high-frequency field distortions along the cord, particularly near the intervertebral junctions.



Supporting Information Figure S5: 2D and 3D multi-echo GRE data in the C-spine and TL-spine at a later echo time compared to the data shown in Figure 7. The TL-spine data presents a single 2D slice acquired during a breath-hold (1mm in-plane resolution; 2mm slice thickness), while the C-spine is imaged during free-breathing in 3D with a 1mm isotropic resolution.